On the precision and accuracy of IGS orbits

Jake Griffiths · Jim R. Ray

Abstract In order to explore the precision and accuracy of International GNSS Service (IGS) orbits, we difference geocentric satellite positions midway between successive daily Final orbits for the period starting November 5, 2006, when the IGS switched its method of antenna calibration, through December 31, 2007. This yields a time series of orbit repeatabilities analogous to the classical geodetic test for position determinations. If we compare our average positional discontinuities to the official IGS accuracy codes, root-sum-squared (RSS) for each pair of days, we find the discontinuities are not well correlated with the predicted performance values. If instead the IGS weighted root-mean-square (WRMS) values from the Final combination long-arc analyses are taken as the measure of IGS accuracy, we find the position differences and long-arc values are correlated, but the long-arc values are exaggerated, particularly around eclipses, despite the fact that our day-boundary position differences apply to a single epoch each day and the long-arc analyses consider variations over a week. Our method is not well suited to probe the extent to which systematic effects dominate over random orbit errors, as indicated by satellite laser ranging residuals, but eclipsing satellites often display the most problematic behavior. A better metric than the current IGS orbit accuracy codes would probably be one based on the orbit discontinuities between successive days.

Keywords GPS · IGS · satellite orbit · accuracy · positional discontinuity · precision

Jake Griffiths (✉)
NOAA/National Geodetic Survey, 1315 East-West Highway, Silver Spring, MD 20910, U.S.A.
tel: +1 301-713-3205
fax: +1 301-713-4324
e-mail: jake.griffiths@noaa.gov

Jim R. Ray
NOAA/National Geodetic Survey, 1315 East-West Highway, Silver Spring, MD 20910, U.S.A.
tel: +1 301-713-2850
e-mail: jim.ray@noaa.gov

1 Introduction

Providing accurate orbit ephemerides for the Global Navigation Satellite Systems (GNSS) has been a core objective of the International GNSS Service (IGS) since its founding in 1994 (e.g., Beutler et al. 1999). Different product series are published for diverse applications; see http://igscb.jpl.nasa.gov/components/prods.html. The Ultra-rapid GPS orbits span 48 hours and are released four times daily with an initial latency of 3 hours. The first half of each Ultra-rapid file is based on fits to observational data while the second half is predicted. These are intended for real-time and near real-time applications. The daily Rapid GPS orbits cover the 24 hours of the previous UTC day with an initial latency of 17 hours. They have near-definitive quality and robustness, and are intended for high-accuracy, rapid-turnaround uses. The Final GPS and GLONASS orbits are the definitive IGS orbital products and are released weekly as a bundle of seven daily files. Special care is taken to ensure the highest level of consistency with the associated IGS terrestrial reference frames, Earth rotation parameters, and receiver and satellite clocks. Consequently, the latency of the Final products is longer, about 13 days or more.

Each IGS orbit product is generated from a weighted linear combination (Beutler et al. 1995) of solutions contributed by up to eight independent Analysis Centers (ACs); see http://igscb.jpl.nasa.gov/organization/centers.html#ac for a list of the IGS ACs. The individual ACs mostly use distinct data reduction systems and procedures, drawing GPS observational data from the IGS global tracking network of more than 300 stations. The Standard Product #3 (SP3) format (Spofford and Remondi 1995) is used to exchange orbital information in the form of tabular ephemerides of satellite positions every 15 minutes expressed in a terrestrial crust-fixed reference frame; see also http://igscb.jpl.nasa.gov/igscb/data/format/sp3c.txt. Associated consistent estimates for the satellite clocks are also provided in the SP3 files at 15-minute intervals. (Since November 2000 the satellite clocks are available in addition at 5-minute intervals, and since January 2007 at 30-second intervals)

The purpose of this report is to assess the precision and accuracy of the IGS Final GPS orbits. The performances of the Rapid and Ultra-rapid orbits are not specifically considered here but our general results and methods should be equally applicable. (The poorer GLONASS orbits, which do not yet form a globally accurate positioning system and for which the IGS analyses are not very robust, are not considered at this time.) The IGS routinely provides internal measures of product accuracy to permit users to apply differential analysis weights for the individual satellites based on their expected orbit quality. In the absence of any alternative independent tracking system of comparable accuracy to the GPS data itself, it is difficult to test the absolute reliability of the IGS accuracy estimates. However, a limited amount of laser ranging tracking data are available and have recently been reanalyzed (Urschl et al. 2007). Those results will be considered here together with day-to-day orbit repeatabilities. We will show that the current IGS internal accuracy metrics are not very discriminating in a relative sense and are almost certainly optimistic in an absolute sense. Alternative strategies to quantify orbit accuracy will be considered.

2 IGS internal orbit accuracy estimates

With all its orbits, the IGS provides estimates of the product quality in the form of "accuracy codes" for each satellite based on the weighted root-mean-square (WRMS) of the differences among the contributing ACs compared to the average orbits. These are published in the header of the SP3 files. Considering the very large and steady improvement in the consistency among IGS AC orbits, shown in Fig. 1, it is timely to reconsider the current level of performance. In the case of the Final orbits, which are produced in seven-day batches, the IGS also computes "long-arc" WRMS residuals for each satellite orbit based on a dynamical fit of the ephemerides over the full week (Beutler et al. 1995); these values are given in the weekly combination summary reports available at http://igscb.jpl.nasa.gov/mail/igsreport/igsreport.html. As an alternative internal measure of the IGS orbit accuracy, we examine a type of geodetic repeatability computed from the differences in geocentric satellite positions (i.e., "positional discontinuities") at the central epoch between successive pairs of daily SP3 files. All three methods are compared to one another, and later with satellite laser ranging (SLR) results for the two GPS satellites with retro-reflectors, PRN05 and PRN06. Following longstanding IGS practice, we will use statistics based on 1-dimensional orbit differences (that is, the average of the three geocentric component differences) rather than the magnitude of the 3-dimensional vector differences.
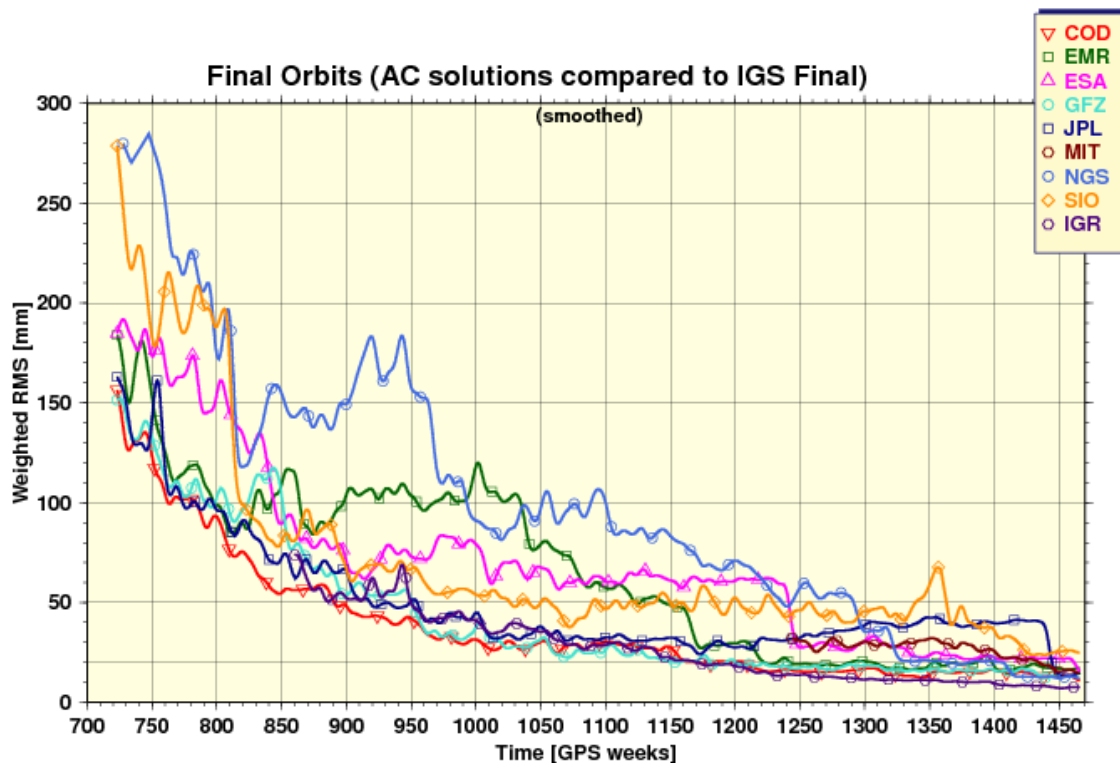

Fig. 1 The WRMS orbit differences (1-D) among IGS Analysis Centers over the history of the organization (from http://www.gfz-potsdam.de/pb1/igsacc/igsacc_final.html courtesy of G. Gendt). A 7-day smoothing has been applied for better visibility. The eight ACs are shown together with the IGS Rapid orbits (IGR), all compared to the combined Final orbits. Recent improvements by JPL are due to the software switch to GIPSY version 5.0.

2.1 IGS "accuracy codes"

The header section of an IGS SP3 orbit file contains rows listing the available satellites in the file and rows listing the corresponding accuracy exponents (Spofford and Remondi 1995). Accuracy exponents (or so-called "accuracy codes") for a given satellite are derived from the weighted RMS orbit agreement among the contributing AC solutions after adjusting a 7-parameter Helmert similarity transformation to account for possible systematic frame differences (Kouba et al. 1995). The result is then expressed, in mm, as the integer base-2 logarithm:

$$\text{AccCode} = \log_2(\sigma) \tag{1}$$

where σ is the formal uncertainty of the combined orbit, given by:

$$\sigma^2 = \frac{\sum_{j=1}^{N} W_j \cdot (RMS_j)^2}{(N-1) \cdot \sum_{j=1}^{N} W_j} \tag{2}$$

and where W_j are the AC weights, N is the number of ACs used, and RMS_j is computed from the AC orbit differences by:

$$(RMS_j)^2 = \sum_{t=1}^{M} \frac{(X_j - \overline{X})_t^2 + (Y_j - \overline{Y})_t^2 + (Z_j - \overline{Z})_t^2}{3M - 7} \tag{3}$$

with $(X_j, Y_j, Z_j)_t$ being the time series of geocentric satellite coordinates for AC j, $(\overline{X}, \overline{Y}, \overline{Z})_t$ the time series of weighted average geocentric satellite coordinates; and M the number of ephemeris epochs from AC j.

Thus, a WRMS orbit residual between 6 and 10 mm is encoded as an "accuracy code" of 3 (i.e., 8 mm). A code of 0 ("accuracy unknown") is assigned when only one AC is available. Note that these are 1-dimensional accuracy estimates and apply for a given satellite over the full span of the particular SP3 file normally consisting of 96 epochs from 0:00 to 23:45. Starting in August 2004, the IGS combined products began to include similar time-dependent accuracy estimates for each satellite coordinate and clock estimate at each 15-minute epoch, computed analogously to that above; see IGS Mails #5000 (http://igscb.jpl.nasa.gov/mail/igsmail/2004/msg00223.html) and #5008 (http://igscb.jpl.nasa.gov/mail/igsmail/2004/msg00231.html). Those time-dependent errors are not very different except when Ultra-rapid predictions are included and so they are not examined here.

The SP3 header section shown in Fig. 2 is an example of accuracy codes for day 1 of GPS week 1420 (Modified Julian Day 54185). Rows 3 and 4 of the header contain a list of the 30 GPS satellites broadcasting signals on 26 March 2007. In rows 8 and 9 are the corresponding accuracy codes, which show that the SP3 positions for satellites PRN19 and PRN29 are the most uncertain (WRMS = 16 mm each) while most of the other

satellite positions have half the error (WRMS = 8 mm each) except that PRN10 and PRN25 are even better (WRMS = 4 mm each).

```
#cP2007  3 26  0  0  0.00000000       96 ORBIT IGS05 HLM   IGS
## 1420  86400.00000000   900.00000000 54185 0.0000000000000
+   30    G01G02G03G04G05G06G07G08G09G10G11G12G13G14G16G17G18
+         G19G20G21G22G23G24G25G26G27G28G29G30G31  0  0  0  0
+          0  0  0  0  0  0  0  0  0  0  0  0  0  0  0  0  0
+          0  0  0  0  0  0  0  0  0  0  0  0  0  0  0  0  0
+          0  0  0  0  0  0  0  0  0  0  0  0  0  0  0  0  0
++         3  3  3  3  3  3  3  3  3  2  3  3  3  3  3  3  3
++         4  3  3  3  3  3  2  3  3  3  4  3  3  0  0  0  0
++         0  0  0  0  0  0  0  0  0  0  0  0  0  0  0  0  0
++         0  0  0  0  0  0  0  0  0  0  0  0  0  0  0  0  0
++         0  0  0  0  0  0  0  0  0  0  0  0  0  0  0  0  0
%c G  cc GPS ccc cccc cccc cccc cccc ccccc ccccc ccccc ccccc
%c cc cc ccc ccc cccc cccc cccc cccc ccccc ccccc ccccc ccccc
%f  1.2500000  1.025000000  0.00000000000  0.000000000000000
%f  0.0000000  0.000000000  0.00000000000  0.000000000000000
%i    0    0    0    0       0       0       0       0        0
%i    0    0    0    0       0       0       0       0        0
/* FINAL ORBIT COMBINATION FROM WEIGHTED AVERAGE OF:
/* cod emr esa gfz jpl mit ngs sio
/* REFERENCED TO IGS TIME (IGST) AND TO WEIGHTED MEAN POLE:
/* PCV:IGS05_1402 OL/AL:FES2004  NONE     Y  ORB:CMB CLK:CMB
```

Fig. 2 Header section of the IGS SP3 orbit file for 26 March 2007. The third and fourth lines contain a list of available GPS satellites for the day. Each GPS satellite number is preceded by the letter "G". The eighth and ninth lines contain the list of accuracy exponents for the corresponding satellites in the third and fourth lines, expressed in a base-2 logarithm system.

It is important to note that the quantization of the WRMS caused by the integer base-2 logarithm encoding means that users of SP3 accuracy codes are limited to the mm values 1, 2, 4, 8, 16, and so forth. We avoid this base-2 quantization limitation here by using the actual WRMS values from the IGS Final orbit combination summary reports. For example, the accuracy codes in Fig. 2 are derived from the values shown for "IGS" in Table 1. (Note that before week 1410 the summary report units were rounded to the nearest cm, but were changed to mm units at the end of January 2007; see IGS Mail #5522 at http://igscb.jpl.nasa.gov/mail/igsmail/2007/msg00002.html.)

2.2 WRMS from IGS "long-arc" analysis

Another estimate of orbit accuracy provided by the IGS is the WRMS from the so-called "long-arc" fit computed as part of the IGS Final orbit combination and reported in the Final weekly summary reports. (There are no comparable fits in the Rapid or Ultra-rapid combinations.) For each AC and IGS combined orbit solution a "long-arc" analysis is performed by fitting the extended CODE orbit model—3 components each of position and velocity plus 9 perturbing accelerations due to solar radiation pressure (Beutler et al. 1994)—to each 7-day time series. In cases where there are no unexpected accelerations, the long-arc fit verifies the day-to-day consistency of each satellite solution. This test is most useful in revealing velocity changes, such as those related to attitude control events, and in isolating problematic AC solutions that are then excluded from the combination.

Table 1. Example of WRMS values from IGS Final orbit combination for day 1 of GPS week 1420 (26 March 2007). Column 1 lists the satellites and flags those undergoing eclipse by "E". Columns 2 through 10 list the WRMS values for each IGS Analysis Center, named in the second row. The rightmost column, "IGS", shows the combined WRMS values for each satellite from which the accuracy codes in Fig. 2 were derived. This example was taken from Table 3.1420.1 of IGS Report #14985 available at http://igscb.jpl.nasa.gov/mail/igsreport/2007/msg00366.html.

```
          Weighted Average  (in mm)
  PRN  |  cod  emr  esa  gfz  igr  jpl  mit  ngs  sio  IGS
 ------+-------------------------------------------------------
    1E |   13   18   24   20   10   22   18   17   32    7
    2  |   17   20   18   21   10   60   27   25   39    9
    3E |   18   19   27   19   11   17   15   22   27    7
    4  |   10   19   22   19    8   12   10   12   34    6
    5  |   12   14   19   21    8   12   16   12   24    6
    6E |   16   21   28   21   11   19   23   18   27    8
    7E |   16   25   29   25   11   19   25   18   44    9
    8  |    7   13   29   15    9   17   17   14   35    6
    9  |   13   11   21   15    7   14   24   11   28    6
   10  |    7   12   17   16    8   12   15   15   23    5
   11  |   17   18   21   25    9   50   23   14   32    8
   12  |   18   21   23   21    9   62   21   17   53    9
   13E |   16   16   23   17   10   54   15   11   20    7
   14E |   13   15   16   12    7   53   13   10   29    6
   16  |   22   17   17   22    7   59   24   15   31    8
   17E |   10   18   22   14    5   55   15   13   36    7
   18  |   17   18   21   23    7   61   20   15   22    8
  X19E |   39  ---  196   28   15  104   20   22   29   16
   20  |   16   17   18   18    8   58   24   12   30    8
   21  |   23   16   24   24    7   83   25   14   27   10
   22  |   16   16   25   23    9   60   18   16   23    8
   23E |   16   13   15   17    7   52   11   11   21    6
   24  |    7   14   20   18    8   12   26   17   29    7
   25  |   12   12   17   16    5   14   12   12   17    5
   26E |   16   12   26   26    8   20   19   16   26    7
   27  |   12   16   23   17    8   17   16   11   39    6
   28  |   13   18   21   23   11   69   23   14   25    8
  X29E |   17   22   51   18   13   35   32   25  ---   11
   30  |   10   13   33   20    5   11   14   12   21    6
   31  |   13   16   19   19    8   61   24   16   30    8
 ------+-------------------------------------------------------
```

Table 2 shows an example of the long-arc WRMS values for day 1 of GPS week 1420, the same day illustrated in Table 1. The column labeled "IGS" is for the combined Final orbits. Satellites PRN19 and PRN29, both in eclipse, have by far the largest long-arc residuals. This is consistent with their larger accuracy codes in Table 1 also, but the differences relative to the other satellites are much greater for the long-arc fits. By contrast, PRN21 has the third largest accuracy code in Table 1 but has one of the smallest long-arc fits in Table 2. Overall, the long-arc residuals are about three times larger than the official accuracy codes. Comparing Tables 1 and 2 it is apparent that they convey distinctive perspectives, but it is not immediately evident which, if either, might provide a better representation of the actual orbit accuracy or precision.

Table 2. Example of long-arc WRMS values for day 1 of GPS week 1420. The organization and source is the same as in Table 1.

```
            Orbit Dynamics (in mm )
  PRN  |   cod  emr  esa  gfz  igr  jpl  mit  ngs  sio   IGS
------+-----------------------------------------------------
   1E |    25   29   35   27   25   26   32   27   32    23
    2 |    19   35   34   33   24   39   31   21   37    23
   3E |    26   28   38   33   29   26   29   39   28    27
    4 |    25   37   29   33   28   32   26   28   30    27
    5 |    30   35   36   36   31   28   36   31   34    30
   6E |    23   35   28   26   28   24   27   25   25    25
   7E |    40   52   56   40   44   46   44   44   56    42
    8 |    25   26   19   28   26   25   27   32   20    22
    9 |    28   33   37   29   30   26   24   28   24    26
   10 |    21   27   26   29   24   27   20   31   35    23
   11 |    26   44   41   37   31   31   28   29   35    29
   12 |    26   40   35   35   26   41   32   23   35    26
  13E |    25   35   40   26   27   31   28   31   27    26
  14E |    40   46   43   38   38   44   36   40   45    39
   16 |    25   40   41   39   29   43   39   30   40    31
  17E |    27   35   38   29   27   32   29   23   31    26
   18 |    23   38   33   33   24   38   25   21   20    22
 X19E |   167  ---  113  159  147   86  133  139  137   143
   20 |    25   39   36   32   28   34   29   28   26    25
   21 |    26   36   33   36   26   50   24   29   26    25
   22 |    24   36   34   32   25   35   21   25   20    23
  23E |    25   34   35   29   28   32   30   34   28    28
   24 |    31   31   31   33   31   30   36   37   33    30
   25 |    27   35   31   28   28   30   28   30   23    27
  26E |    25   32   46   36   27   30   28   28   32    28
   27 |    27   26   26   29   27   24   29   30   20    24
   28 |    22   36   34   36   29   34   29   26   26    24
 X29E |   109  114   98  107  107  110  109  106  ---   105
   30 |    30   36   42   37   31   27   33   28   30    29
   31 |    23   39   38   37   31   41   31   30   33    29
------+-----------------------------------------------------
```

2.3 Comparison of IGS accuracy estimates

Fig. 3 illustrates the time variation of the IGS accuracy codes and long-arc fits for PRN01 over the period from GPS week 1400 through 1457. The examination starts with week 1400 (5 November 2006) because the IGS changed its basic calibration model for satellite and tracking antennas at that time (Schmid et al. 2007). Recall also that the quantization unit for IGS reports changed from 1 cm to 1 mm starting GPS week 1410, which explains the improved plot resolution at that time. Earth ("E") and lunar ("M") eclipse periods are indicated. The PRN01 accuracy codes are nearly constant (between 5 and 10 mm), but the long-arc WRMS values vary dramatically, especially during eclipse seasons. Similar patterns are also seen for the other GPS satellites.

PRN 01, Block II-A, Plane F, Slot 1
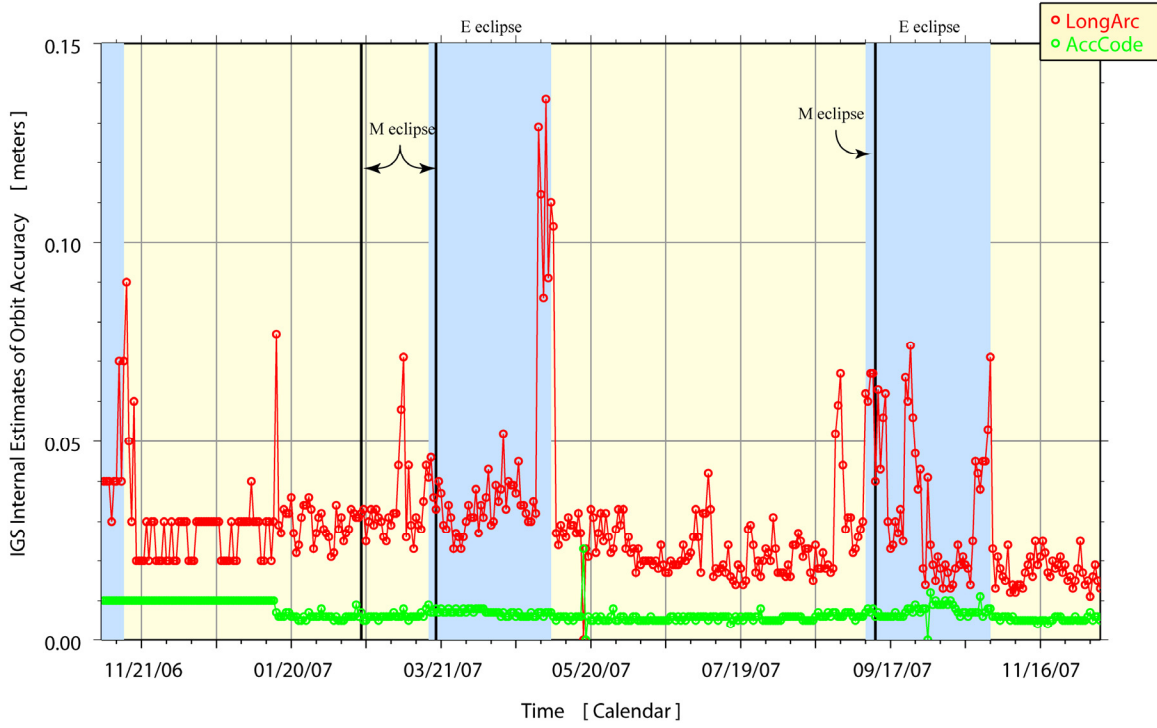
Fig. 3 Time series of accuracy-code (AccCode) and long-arc (LongArc) WRMS values for PRN01 extracted from the IGS Final summaries (http://igscb.jpl.nasa.gov/mail/igsreport/igsreport.html). The plot period covers day 0 of GPS week 1400 (5 November 2006) to day 3 of week 1457 (12 December 2007). The blue shaded vertical bands mark Earth eclipse intervals, when the satellite is sometimes shaded from the sun by the Earth, and the three thick, vertical black lines denote lunar eclipse intervals, when the satellite is sometimes shaded from the sun by the moon. The change in IGS report quantization from 1 cm to 1 mm units is seen at MJD 54114.

3 SP3 "positional discontinuities"

As an alternative to the two IGS accuracy estimates discussed above, we consider a statistic analogous to classical geodetic position repeatability. Since satellite trajectories are not sufficiently stationary, however, simple repeatability is not adequate, even allowing for Helmert transformations. Instead, let us compute the magnitude of the 1-D shift in the geocentric (terrestrial crust-fixed frame) satellite positions from the end of one SP3 orbit to the beginning of the next. This "positional discontinuity" is defined as:

$$ PD = \frac{|X_B - X_A| + |Y_B - Y_A| + |Z_B - Z_A|}{3} \tag{4} $$

where subscript "A" denotes the coordinates from the first orbit file and "B" those of the second. Such a difference only makes sense if the epoch of the two sets of coordinates is the same, a condition not satisfied by the IGS SP3 products, which end at 23:45 for each daily file and begin with 00:00 for the next. On the other hand, if the IGS orbits used longer spans of observational data and overlapped, making the PD computation easy, then the results would not be independent from one day to the next. In that case, the PD

differences would under-represent the actual orbit errors. An extreme example of this type would be the forced continuity of orbits between daily arcs. In fact, some IGS ACs do use overlapping GPS datasets or multi-day satellite arcs, although velocity breaks are inserted every 12 hours (or some other stochastic process is invoked). Those contributions will tend to reduce the daily orbit discontinuities in the IGS combined products to some extent.

In order to match endpoint epochs between successive SP3 orbit files, we implemented a fitting and extrapolation procedure using the same extended CODE orbit model (Beutler, et al. 1994) used for the IGS long-arc analysis. The IGS SP3 positions were fitted as pseudo-observations by minimizing the residuals to the extended CODE model using a standard orbit integration procedure. The procedure, illustrated in Fig. 4, is as follows:

- fit the orbit model to the SP3 positions for day "A" and extrapolate forward from 23:45 by 7.5 minutes to epoch 23:52:30 of day "A";
- then fit the orbit model to the SP3 positions for day "B" and extrapolate backward from 00:00 by 7.5 minutes to 23:52:30 of day "A";
- finally, difference the geocentric positions using Eq. (4).

It should be obvious that these orbit offsets can provide some insight into the precision of IGS orbits, but they cannot detect such systematic biases as a global scale (i.e., radial) error. So we will only address the lower limits for IGS orbit accuracy.
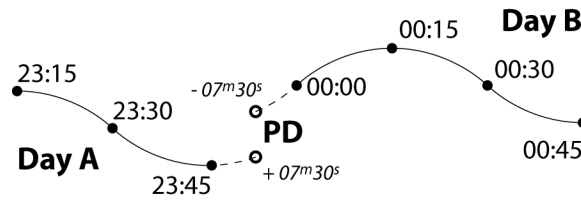

Fig. 4 Illustration of the computation of the positional discontinuity (PD) in the satellite orbits between two successive SP3 daily files. The orbit fitting and extrapolation is done using the extended CODE orbit model.

A positional discontinuity, by definition, uses information from adjacent days "A" and "B" whereas the IGS internal accuracy estimates apply to individual days. Thus, to compare positional discontinuities with IGS accuracy estimates some adjustment is necessary. For this study we convolve the accuracy estimates from days A and B using a root-sum-square and refer to the resulting as RSS WRMS (or RWRMS) values, as shown in Fig. 5 for PRN01.

The IGS policy is to track all active GPS satellites regardless of the official "health bits" set in the broadcast navigation message. For our purposes here, we consider all satellites with a non-zero accuracy code to be healthy. An accuracy code of 0 usually implies that the satellite was maneuvered by the GPS operations and control center at Schriever Air Force Base in Colorado. Clock maintenance is not a reason for us to omit a satellite, as that has no effect on the orbit quality.

Examining the time series plot in Fig. 5, it is apparent that, for PRN01, the positional discontinuities are intermediate between the accuracy code and long-arc RWRMS values; the temporal variations appear largely unrelated. The long-arc variations are especially sensitive to eclipsing, while the official accuracy codes hardly change during eclipses.

The apparent independence of the positional discontinuities for PRN01, in fact, is evident for all the healthy GPS satellites as illustrated in Fig. 6. Correlation of the positional discontinuities with either the accuracy code or long-arc RWRMS values would show as a cloud of points trending along the diagonal lines in Figs. 6a and 6b, respectively. Instead, the cloud of points in Fig. 6a trends horizontally, emphasizing the fact that the accuracy code values are essentially constant over time and do not resolve differences between satellites. For the long-arc fits, the cloud of points in Fig. 6b is diffuse, but a linear regression suggests there is a trend at a slope about 1.7 times that of the line shown. So, although the long-arc values vary and may resolve differences among satellites, they are exaggerated with respect to the positional discontinuities.

PRN 01, Block II-A, Plane F, Slot 1
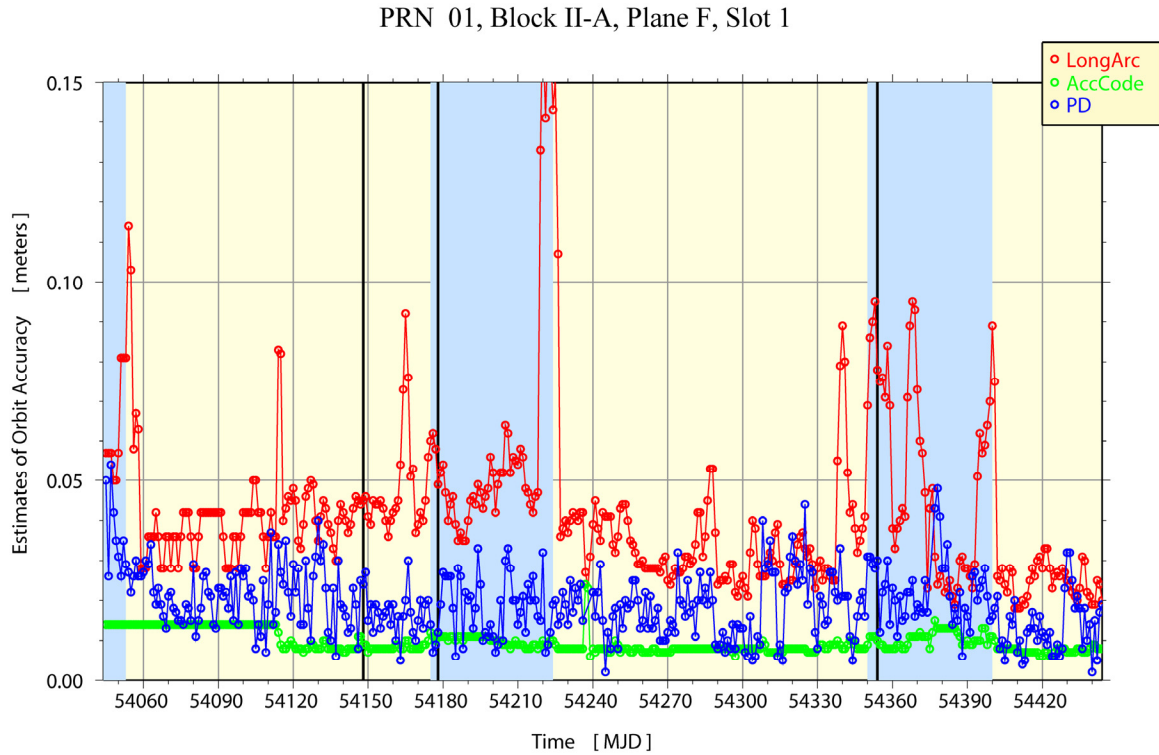
Fig. 5 Time series of positional discontinuities (PD, in blue) for PRN01 compared with the equivalent accuracy-code RWRMS (in green) and long-arc RWRMS (in red) values.

We recognize that our fitting and extrapolation procedure is a likely source of error separate from the intrinsic uncertainty in the IGS orbits. In order to estimate an upper limit on the error, we mimic the fitting/extrapolation process illustrated in Fig. 4 by:

- fitting the orbit model to the SP3 positions from 00:00 to 23:45 on "A";
- then fitting from 00:00 to 23:30, dropping the 23:45 epoch, on the same day and extrapolating to 23:45;
- finally, differencing the geocentric positions at 23:45 using Eq. (4) to get the so-called "test differences".

According to these test differences, the 1-D error introduced by the fitting and extrapolation process adds about 8 mm of noise compared to the average observed discontinuities of 21 mm (Table 3). So the fitting/extrapolation process adds only minor noise to the positional discontinuities. In fact, this test of the fit noise is pessimistic

because the extrapolation interval is double that used for the orbit discontinuities. For short spans, orbit extrapolation errors probably grow at least linearly. On the other hand, the PD values involve errors for two independent days. As a result, our fit test error is likely too large by roughly $\sqrt{2}$.

a.

b.
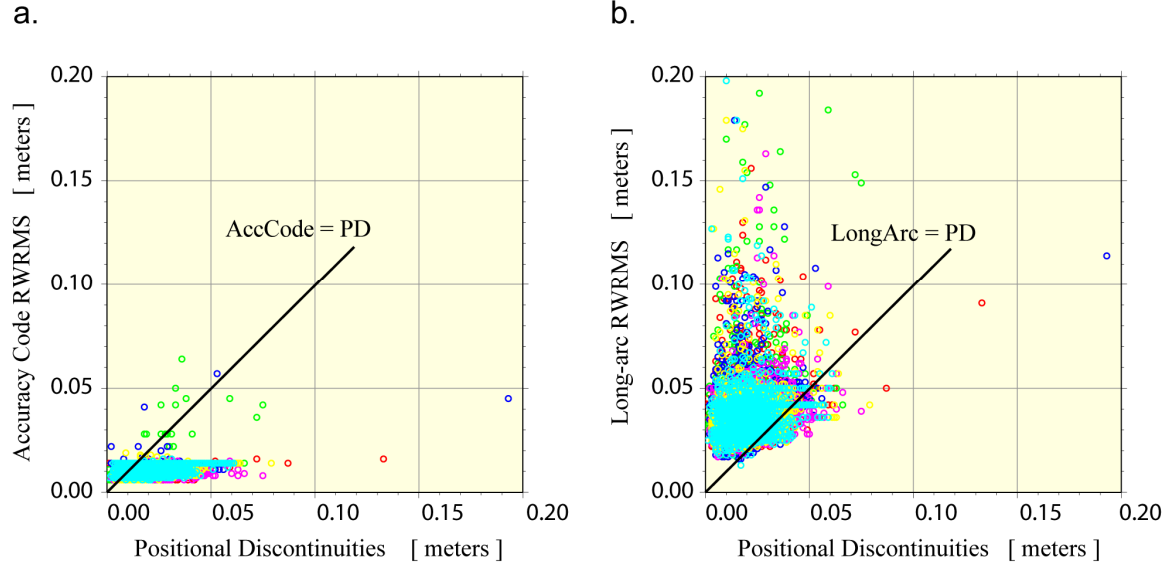
Fig. 6 In (a), comparison of all the accuracy code RWRMS values and positional discontinuities for all healthy GPS satellites for the period November 5, 2006 through December 31, 2007. In (b), comparison of all the long-arc RWRMS values and positional discontinuities for the same time frame as those in (a). Eclipses are omitted. Different colors are used for the six different orbital planes, but there seems to be no obvious relationships.

From Table 3, one can see little indication of large performance differences among satellites. However, it is curious that the older generation of Block IIA satellites do seem to yield more precise orbits (average ≈ 19 mm) than the IIR and current IIR-M satellites (average ≈ 22 mm), though the difference might not be significant. Given the improved attitude control of the post-IIA spacecraft, this observation is unexpected, but other block design changes (e.g., solar panel redesign and increased mass) could be more important.

4 Discussion

4.1 Orbit accuracies and SLR range residuals

SLR is used to track the distance, or range, between a laser station and a satellite. Differences between the observed SLR ranges and the ranges computed from GPS orbits are called range residuals. Urschl et al. (2007) derived range residuals for the two GPS satellites equipped with SLR retro-reflectors, namely PRN05 and PRN06. The range residuals were derived using final orbit products from the IGS and three Analysis Centers (CODE, GFZ and JPL). (Note that the SLR tracking data are too sparse to compute full 3-D orbits, so only radial comparisons are feasible.)

Table 3 Statistics for positional discontinuities and test differences, ignoring eclipses, organized by satellite block and launch date.

| Launch MJD	Satellite	Mean (mm) PD	PD σ (mm)	Mean (mm) Fit Error	Fit Error σ (mm)
Block IIA:					
48441	PRN24	21.3	11.1	6.3	3.5
48675	PRN25	18.7	9.3	5.9	3.9
48810	PRN26	18.3	9.0	8.8	5.4
48874	PRN27	18.3	9.9	6.0	3.4
48948	PRN01	19.3	8.3	7.2	3.8
49120	PRN07	20.0	11.3	7.6	3.8
49164	PRN09	18.3	8.6	7.4	4.5
49229	PRN05	16.8	8.5	6.6	4.8
49286	PRN04	24.3	13.6	7.7	4.3
49421	PRN06	19.3	8.7	7.4	3.7
50170	PRN03	19.2	12.5	6.6	4.2
50280	PRN10	19.4	10.2	7.5	3.8
50338	PRN30	16.8	9.3	6.2	4.3
50758	PRN08	19.0	11.0	6.1	3.8
average	IIA	19.2	10.1	7.0	4.1
Block IIR:					
50652	PRN13	22.2	12.5	9.8	5.8
51458	PRN11	24.6	9.4	7.9	4.4
51675	PRN20	20.2	12.2	7.5	4.5
51741	PRN28	21.4	15.0	6.2	4.9
51858	PRN14	21.1	15.3	8.1	3.8
51939	PRN18	20.9	9.0	9.5	5.7
52668	PRN16	20.5	8.7	10.7	6.3
52729	PRN21	21.3	8.2	10.1	5.3
52994	PRN22	22.8	8.7	9.7	5.1
53084	PRN19	21.9	22.6	8.2	4.5
53179	PRN23	22.5	14.3	10.5	6.0
53315	PRN02	19.7	9.1	8.4	4.4
average	IIR	21.6	12.1	8.9	5.1
Block IIR-M:					
53639	PRN17	21.1	11.5	6.6	3.9
54003	PRN31	22.7	11.1	10.4	6.9
54056	PRN12	22.3	9.6	6.8	4.3
average	IIR-M	22.0	10.7	7.9	5.0
average	all	20.9 ± 2.0	11.0	7.9 ± 1.5	4.7

In Figs. 7 and 8, we compare the IGS internal accuracy estimates, our positional discontinuities as estimates of orbit accuracy and the standard deviation, $\sigma_{SLR\text{-}GPS}$, of the range residuals from Urschl et al. (2007) for PRN05 and PRN06, as shown in Figs. 7 and 8. One must consider whether the laser range residuals really are comparable with our various 1-D GPS accuracy metrics, which involve comparisons between two successive

days. If the laser range differences are affected by roughly similar levels of errors due to the SLR technique and the GPS orbits, then we assert that the comparisons in Figs. 7 and 8 are indeed comparable, at least approximately, though for different reasons. We do not consider the mean range biases found by Urschl et al. (2007)—31 and 28 mm, respectively. Some portion of the range biases is likely due to errors in the assumed offsets between the retro-reflectors and the satellite centers-of-mass (e.g., Urschl et al. 2007); for the current best estimates, see SLR Mail #1481 (ftp://ftp.dgfi.badw-muenchen.de/pub/laser/messages/slrmail).

In Fig. 7, the standard deviation, $\sigma_{SLR\text{-}GPS}$, of the SLR range residuals is 19 mm and the average positional discontinuity is 17 mm, whereas the average accuracy code and long-arc RWMRS values are 9 mm and 42 mm, respectively. Similarly in Fig. 8, the standard deviation, $\sigma_{SLR\text{-}GPS}$, for the SLR residuals is 25 mm and the average positional discontinuity is 19 mm; the average accuracy code and long-arc RWMRS values are 9 mm and 96 mm, respectively.

PRN 05, Block II-A, Plane B, Slot 5
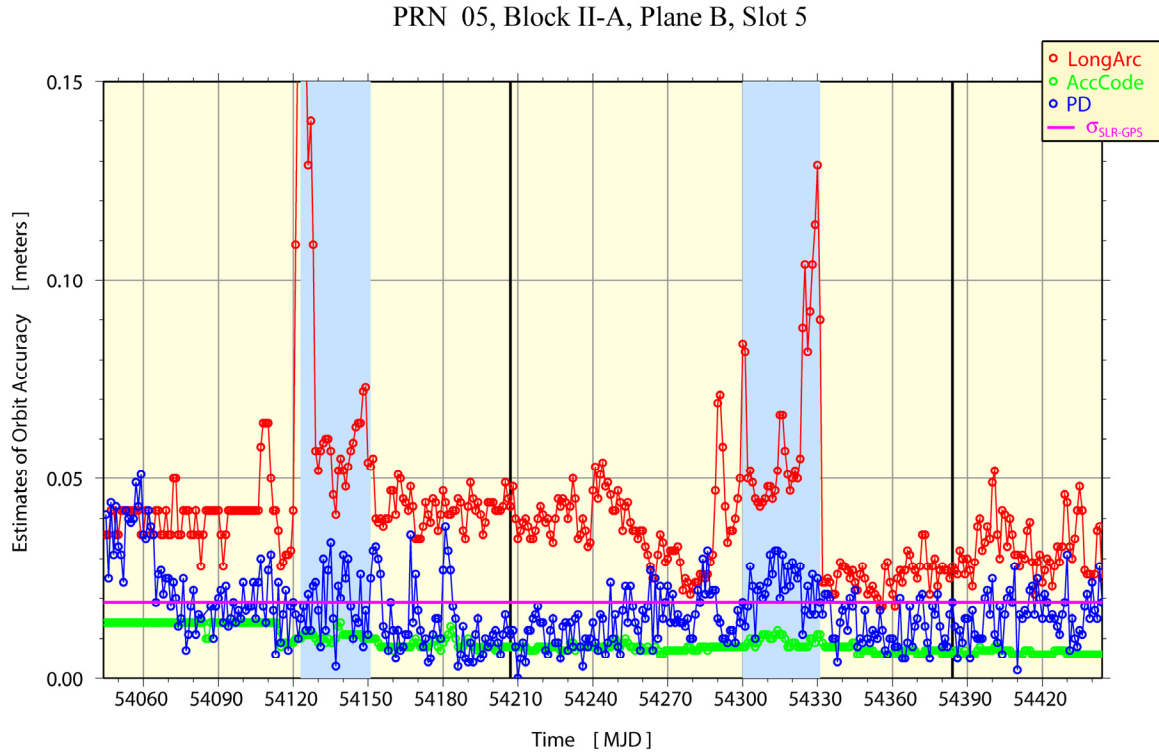
Fig. 7 Time series of positional discontinuities (PD, in blue), and accuracy-code RWMRS (in green) and long-arc RWMRS (in red) values for PRN05. The magenta line represents the standard deviation of the SLR range residuals, derived from IGS Final orbits, for PRN05 (Urschl, et al. 2007).

PRN 06, Block II-A, Plane C, Slot 1
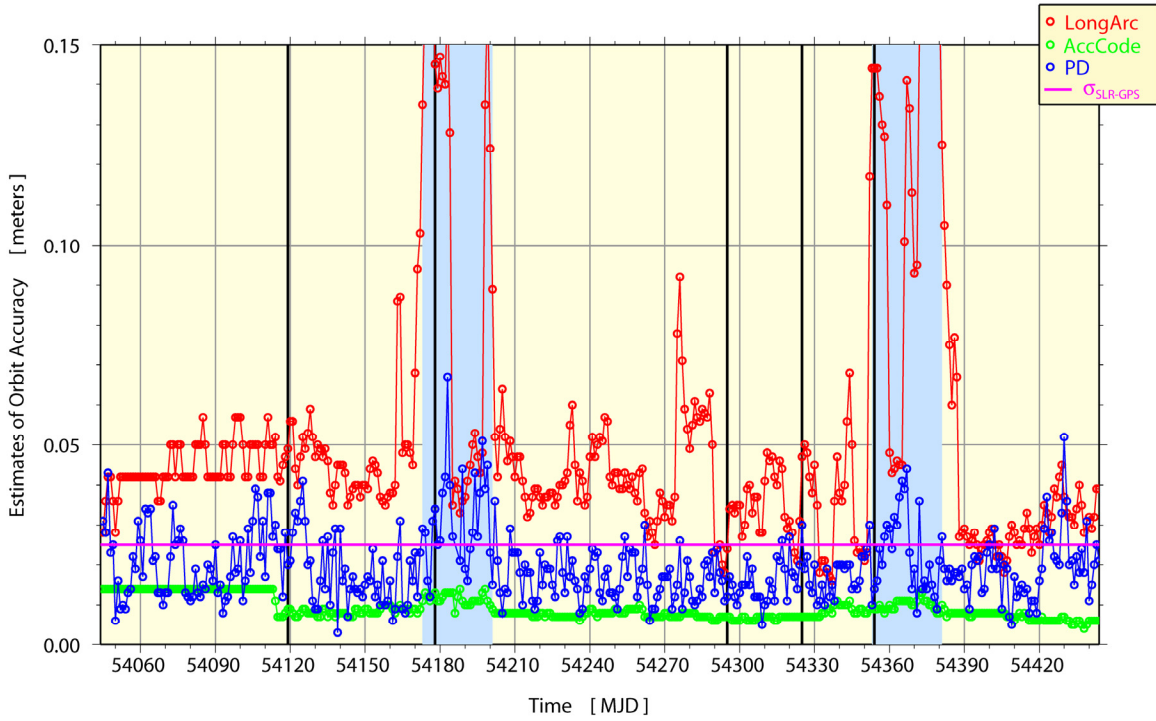
Fig. 8 Same as Fig. 7 except for PRN06.

For PRN05 and PRN06, it is clear that the average positional discontinuities are roughly consistent with the standard deviations of the SLR range residuals, much more so than the IGS internal accuracy estimates. The positional discontinuities also seem to reflect variations in performance among satellites and over time, such as during Earth eclipse periods (e.g., review Figs. 5, 7 and 8), especially when the eclipsing happens across the day boundary.

The magnitude of a positional discontinuity, however, may occasionally be small due to fortuitously good agreement for a satellite orbit between two successive SP3 files. This is likely the case for the occasional small magnitudes shown in Figs. 5, 7 and 8. If positional discontinuities were to be used as orbit accuracy estimates in practice, such small, unrealistic magnitudes would lead to overly optimistic estimates of accuracy. Therefore, one should devise a mechanism, such as a root-sum-square error floor, to avoid overly optimistic accuracy estimates before using the orbit jumps as an operational measure of precision or accuracy.

4.2 Periodicities in the SP3 positional discontinuities

Fig. 9a (red line) shows the power spectrum of the positional discontinuities, computed by a standard fast Fourier transform method. Sparse data gaps have been filled using linear interpolation. In order to reduce the spectral noise and search for common-mode signals, spectra for all satellites have been stacked then averaged at each frequency step. A comparable spectrum for the test fit error offsets is shown in Fig. 9b (blue line). (Note that the spectra for individual orbital planes are not distinguishable from the combined constellation spectrum.)

The spectrum of the orbit discontinuities (Fig. 9a) shows a pronounced broad peak near fortnightly periods (around 0.0714 cycles per day) against a background of declining power with frequency, indicative of temporally correlated orbit errors. The overall continuum could be consistent with the power-law behavior of a flicker frequency noise process (illustrated in Fig. 9 by the dashed diagonal line), commonly seen in the spectra of GPS station time series (e.g., Williams et al. 2004), but the lower frequencies are poorly resolved. If there is a high-frequency white noise floor it is not obvious and does not seem important. The test fit errors have a somewhat similar spectrum, but with much less power. The fortnightly peak in the error spectrum is considerably broader than in the orbit discontinuities. So, while the fitting process could contribute slightly to the fortnightly orbit errors, this is unlikely to be the primary agent. In support of this view, note that there is also a weekly peak in the error spectrum at 0.143 cpd (or 7-day period) which is not visible in the orbit spectrum. The fit errors also become predominantly white for periods shorter than about 5 days.
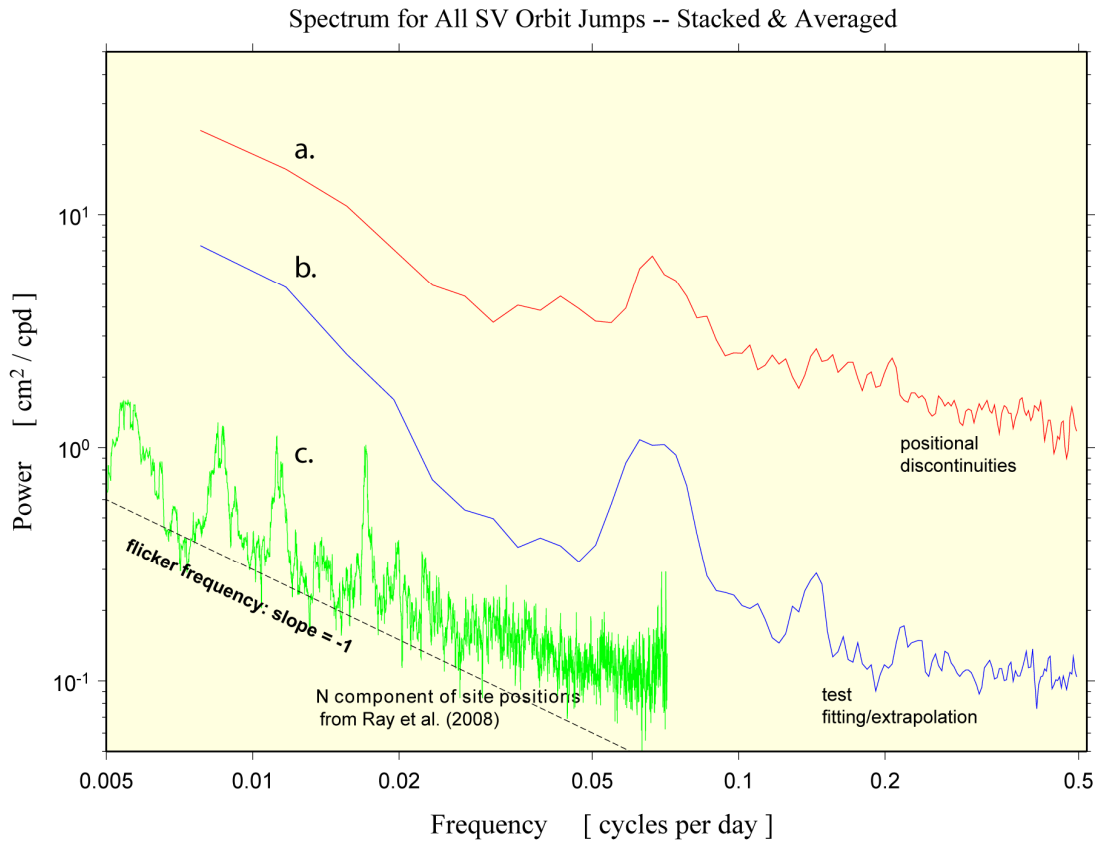
Fig. 9 Spectra derived from **(a)** the SP3 positional discontinuities (in red), **(b)** estimates of error due to the fitting and extrapolation used to estimate the positional discontinuities (in blue) and **(c)** from the local north (N) component of the GPS station positions (in green). The weekly position time series in (c) used 167 global IGS stations with data between 1996 and 2006 (Ray et al. 2008). The site position spectrum has been shifted for visibility so only the relative power variations are consistent with the ordinate scale.

For comparison, the stacked, smoothed spectrum of weekly N position components from 167 IGS global stations is included in Fig. 9c (from Ray et al. 2008). The GPS data

were collected between 1996 and 2006. Spectra for the E and U components are similar, and all three components showed anomalous harmonics at multiples of 1.040 cycles per year (cpy) up to at least 6.24 cpy. There does not appear to be any correspondence between the position harmonics of 1.040 cpy and features in the orbit spectrum, although poor resolution in the orbit results for frequencies in the sub-monthly range could be responsible. There could be some common variation near fortnightly periods in the orbits and station positions, but this is at the Nyquist limit for the latter measurements. Further investigation is needed to confirm anything more than a coincidental link, although it is not surprising to see fortnightly errors in GPS results of all types considering the large tidal effects at this period, which have pervasive impacts throughout the data analysis.

5. Conclusions

The discontinuities in orbit positions between consecutive days imply current IGS orbit precision and accuracy to be greater than or equal to about $21/\sqrt{2} = 15$ mm (1-D global average) for each daily arc. The variation among satellites ranges from about $17/\sqrt{2} = 12$ mm to about $25/\sqrt{2} = 18$ mm, while being worse than average during eclipses. We also find our positional discontinuities are roughly consistent with SLR ranging residuals for PRN05 and PRN06 (19 and 25 mm in the radial component), considering some part must be due to SLR ranging errors (systematic and random).

Current IGS accuracy codes are unrealistically optimistic, 7.3 ± 0.5 mm (1-D global average), and are approximately constant, nearly independent of satellite and time. IGS Final long-arc fits are often overly pessimistic, especially during eclipses due to the harmonic fit over 7 days.

The orbit discontinuities show a prominent fortnightly variation, as do our test differences to evaluate the fit error, though much smaller in amplitude. This signal could be related to fortnightly errors in weekly station coordinate time series (albeit Nyquist limited), for which a variety of tidal effects could be implicated. The overall spectrum of orbit differences decreases in power with increasing frequency consistent with temporally correlated errors, as seen similarly in station position time series.

For practical purposes, positional discontinuities seem to provide the best available estimates for IGS orbit precision and we recommend using them to replace current IGS SP3 accuracy codes, while recognizing the need for some mechanism to avoid sometimes unrealistically small values, such as an RSS noise floor based on the recent past. It is important to note that proposals to force continuity of IGS products across day boundaries are misguided. Such an approach would prevent internal error studies like this one, would only hide errors not eliminate them, would force the orbit errors into other parameters and would increase temporal correlations.

Acknowledgements

References

Beutler G, Brockmann E, Gurtner W, Hugentobler U, Mervart L, Rothacher M (1994) Extended orbit modeling techniques at the CODE Processing Center of the International GPS Service for Geodynamics (IGS): Theory and initial results. Manuscr Geodaet 19: 367-386

Beutler G, Kouba J, Springer T (1995) Combining the orbits of the IGS Analysis Centers, B Geod, 69, 200-222

Beutler G, Rothacher M, Schaer S, Springer T, Kouba J, Neilan RE (1999) The International GPS Service (IGS): an interdisciplinary service in support of earth sciences. Adv Space Res, doi 10.1016/S0273-1177(99)00160-X, 23(4): 631-653

Kouba J, Mireault Y, Lahaye F (1995) 1994 IGS orbit/clock combination and evaluation, Appendix 1 of the Analysis Coordinator report, International GPS Service for Geodynamics 1994 Annual Report, Jet Propulsion Laboratory publication 95-18, 70-94

Press WH, Teukolsky SA, Vetterling WT, Flannery BP (2001) Numerical recipes in Fortran 77: the art of scientific computing (2nd edition). Vol. 1 of Fortran numerical recipes. Cambridge University Press, Cambridge, MA, 992 pp

Ray J, Altamimi Z, Collilieux X, Van Dam T (2008) Anomolous harmonics in the spectra of GPS position estimates. GPS Solut, doi 10.1007/s10291-007-0067-7, 12(1): 55-64

Schmid R, Steigenberger P, Gendt G, Ge M, Rothacher M (2007) Generation of a consistent absolute phase-center correction model for GPS receiver and satellite antennas. J Geod, doi 10.1007/s00190-007-0148-y, 81(12): 781-798

Spofford PR, Remondi BW (1995) The National Geodetic Survey standard GPS Format SP3. NOAA, National Geodetic Survey, ftp://igscb.jpl.nasa.gov/igscb/data/format/sp3_docu.txt

Urschl C, Beutler G, Gurtner W, Hugentobler U, Schaer S (2007) Contribution of SLR tracking data to GNSS orbit determination. Adv Space Res, doi 10.1016/j.asr.2007.01.038, 39(10): 1515-1523

Williams SDP, Bock Y, Fang P, Jamason P, Nikolaidis RM, Prawirodirdjo L, Miller M, Johnson DJ (2004) Error analysis of continuous GPS position time series. J Geophys Res, doi 10.1029/2003JB002741, 109: B03412